

## Study on Dual-Concentric-Core Dispersion Compensation Photonic Crystal Fiber

Zhao-yuan Song\*

Key Laboratory of Metastable Material Science & Technology, Yanshan University, Qinhuangdao 066004, China  
Institute of Infrared Optical Fibers and Sensors, Yanshan University, Qinhuangdao 066004, China and  
College of Science, Liaoning University of Petroleum & Chemical Technology, Fushun 113001, China

Lan-tian Hou

Key Laboratory of Metastable Material Science & Technology,  
Yanshan University, Qinhuangdao 066004, China and  
Institute of Infrared Optical Fibers and Sensors, Yanshan University, Qinhuangdao 066004, China

Xing-tao Zhao, Dong-bin Wei, Xiao-dong Liu, and Zhao-lun Liu

Institute of Infrared Optical Fibers and Sensors, Yanshan University, Qinhuangdao 066004, China  
(Received on 23 April, 2008)

The dual-concentric-core photonic crystal fiber composed of pure silica and air is proposed in this paper. Around 1.55  $\mu\text{m}$ , it exhibits a negative chromatic dispersion as high as -5850 ps/km/nm. Based on multipole method, a systemic and in-depth simulation is realized to investigate the mode characteristics. The explanations to propagation states of the fundamental mode and the second mode are given elaborately. Finally, the variation of structural parameters is investigated to evaluate the tolerance of the fabrication. As a result, the designed fiber can be fabricated easily.

Keywords: Dual-concentric-core photonic crystal fiber; Dispersion compensation; Multipole method

### I. INTRODUCTION

Chromatic dispersion is one of the most fundamental characteristics of optical fiber. The pulse is broadened mostly because of this factor. At present, millions of kilometers of installed optical links around the world operate with 1.31  $\mu\text{m}$  optimized G.652 type of single-mode fibers. Due to the availability of the erbium-doped fiber amplifiers (EDFA) and also because of lower loss at the 1.55  $\mu\text{m}$  band, there has been a substantial interest to operate these installed fibers at the 1.55  $\mu\text{m}$  band. Unfortunately, when operated at the 1.55  $\mu\text{m}$  band these fibers exhibit chromatic dispersion of 16–18 ps/km/nm. In a long-haul optical link, the chromatic dispersion will increase with the propagation distance increasing. Thus some dispersion compensation fibers (DCFs) should be inserted [1] in order to decrease this accumulating dispersion.

Recently, because the structure design of the photonic crystal fiber (PCF) is flexible and dual-concentric-core fiber (DCCF) could attain high negative dispersion easily, some investigations of dual-concentric-core photonic crystal fiber (DCCPCF) [2-12] have attracted considerable attentions.

### II. ANALYSIS METHOD AND STRUCTURE DESIGN

Recently, the multipole method (MPM) [13-14] has become maturity. It is suitable to calculate the PCFs with circle air holes. Such as chromatic dispersion and mode characteristics of PCFs can be well researched. The main idea of MPM is, in the cylinder 1, the mode field is expanded by

Fourier-Bessel function.

$$\Psi_z = \sum_{m=-\infty}^{\infty} a_m^{(l)} J_m(k_{\perp}^i r_l) \exp(im\phi_l) \exp(i\beta z) \quad (1)$$

And in the vicinity of cylinder 1, the mode field is also expanded by Fourier-Bessel function.

$$\Psi_z = \sum_{m=-\infty}^{\infty} \left[ b_m^{(l)} J_m(k_{\perp}^e r_l) + c_m^{(l)} H_m^l(k_{\perp}^e r_l) \right] \exp(im\phi_l) \exp(i\beta z) \quad (2)$$

Here,  $k_{\perp}^i = (k_0^2 n_i^2 - \beta^2)^{1/2}$ ,  $k_{\perp}^e = (k_0^2 n_e^2 - \beta^2)^{1/2}$ .  $n_i$  and  $n_e$  are the refractive indices of air and silicon.  $k_0$  is free space wave vector. The  $r_l$  and  $\theta_l$  are polar value, which are near to the center 1 of the air holes.  $a_m^{(l)}$ ,  $b_m^{(l)}$  and  $c_m^{(l)}$  are matrix coefficients.

On the boundary of 1, by using electromagnetic condition, we can obtain the expression of  $a_m^{(l)}$ ,  $b_m^{(l)}$  and  $c_m^{(l)}$ . The mode propagation constant  $\beta$  and mode field distribution can be obtained using this algorithm. The mode's refractive index of PCF can be obtain as  $n_{eff} = \beta/k$ . In this way, the chromatic dispersion  $D$  is defined as the function of the wavelength  $\lambda$ .

$$D(\lambda) = -\frac{\lambda}{c} \frac{d^2 R_e[n_{eff}]}{d\lambda^2} \quad (3)$$

To obtain a very high dispersion, lots of designs have been proposed, such as W-model, multi-cladding model, dual-concentric-core model [2-12] and so on. However, the dual-concentric-core model does better than the others. Based on this model, many works have been carried through to try to attain large negative dispersion. The first conventional DCCF with D of -100 ps/km/nm around 1.55  $\mu\text{m}$  was proposed in document [2]. In [3-6], D were attained -900 ps/km/nm, -1800 ps/km/nm, -5100 ps/km/nm respectively at 1.55  $\mu\text{m}$  by optimizing structural parameters. In recent years, along with the emergence of PCF, a novel type of DCCF based on PCF is appeared. It has a high index inner core

\*Electronic address: zysong815@163.com

and a defect ring of reduced holes diameter in the cladding. Researchers simulate and design this kind of fiber, and have attained very high negative dispersion [7-12]. However, such high refractive index doping is difficult to realize and high doping of the core is the increasing loss due to higher GeO<sub>2</sub>. Ni Yi et al. have proposed a novel dual-core DCF with D as large as -18000 ps/km/nm [12]. Six small holes were introduced in the core of simple triangular PCF. However, it is difficult to fabricate the fiber exactly according to the design because it adopts a ring of much smaller holes and the accuracy of the structure parameter is difficult to control.

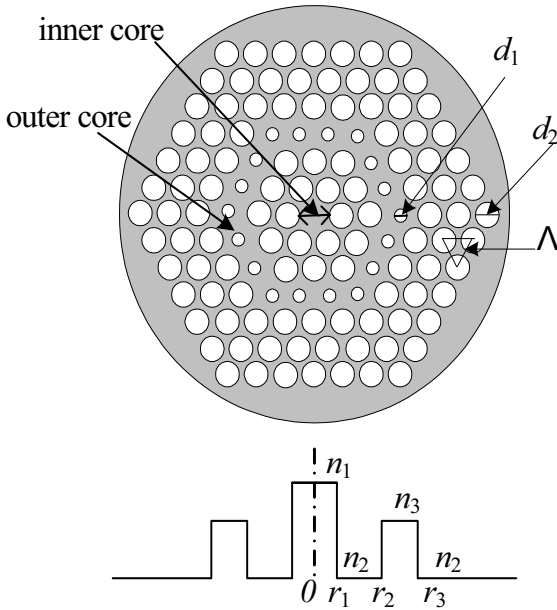


FIG. 1: The cross section and effective index profile of DCCPCF

In this paper, MPM is used to investigate the chromatic dispersion and mode characteristics of DCCPCF. And detailed explanations about the propagation characteristics have been given. The cross section and effective index profile of DCCPCF are shown schematically in Fig. 1. It is obtained by introducing two kinds of holes with different diameters. The large hole's diameter is  $d_1$ , and the small hole's diameter is  $d_2$ . The pitch is  $\Lambda$ . The inner core is surrounded by the six large holes, and the outer core is consisted by the smaller holes. Here, the structural parameters  $\Lambda=1.3 \mu\text{m}$ ,  $d_1=1.0 \mu\text{m}$ ,  $d_2=0.48 \mu\text{m}$  are used in this paper.

### III. NUMERICAL SIMULATION AND ANALYSIS

Due to the special structure of the DCCPCF, it determines there are at least two supermodes in the inner core and the outer core, respectively. One is fundamental mode, and the other is second mode. Typical field patterns in the two cores are shown in Fig. 2.

Fig. 3 shows the relations between the effective indices of the fundamental mode and the second mode versus wavelength, and the relations between the effective indices of the modes in the inner core and outer core versus wavelength.

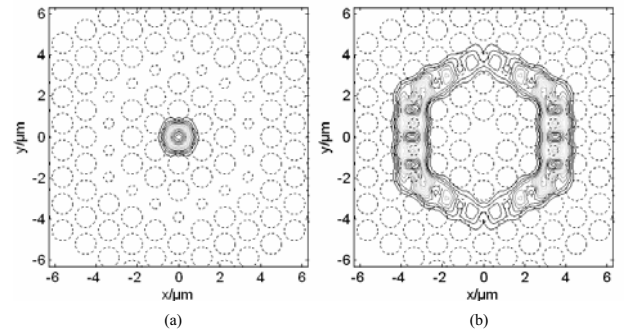


FIG. 2: Typical field patterns in these two cores; (a) In the inner core; (b) The outer core.

Solid and dashed curves correspond to  $n_{eff}$  of the fundamental mode and the second mode, respectively. And the curves marked by circle and square correspond to  $n_{eff}$  of the modes in the inner core and outer core, respectively. From Fig. 3, it could be found that the curves marked by circle and square intersect at a certain wavelength. The cross point corresponds to the phase matching wavelength  $\lambda_p$ . In the Fig. 3,  $\lambda_p=1.548 \mu\text{m}$ . Around  $\lambda_p$ ,  $n_{eff}$  of the modes in the inner core and outer core match to each other, and optical coupling takes place between the modes in the inner core and outer core. At wavelengths shorter than  $\lambda_p$ , the effective indices of the fundamental mode and the second modes are very close to those of the modes in inner core and outer core respectively. At wavelengths longer than  $\lambda_p$ , however, the effective indices of the fundamental mode and the second mode are very close to those of the modes in outer core and inner core respectively.

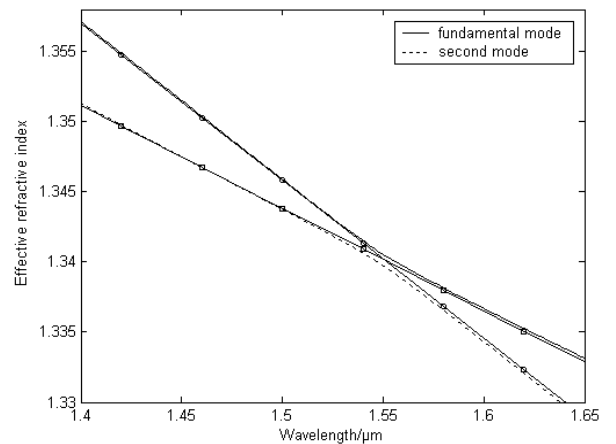


FIG. 3: Relations of the effective indices versus wavelength (Curves marked by circle and square correspond to  $n_{eff}$  of the modes in inner core and outer core)

Table 1 illustrates the effective indices of the fundamental mode and the second mode with wavelength from  $1.40 \mu\text{m}$  to  $1.65 \mu\text{m}$ . It can be seen from Table 1 that, when wavelengths shorter than  $\lambda_p$ , indices of the fundamental mode equal to those of mode in the inner core, and indices of the second mode equal to those of mode in the outer core. However,

when wavelengths longer than  $\lambda_p$ , indices of the fundamental mode equal to those of mode in the outer core, and indices of the second mode equal to those of mode in the inner core.

TABLE 1: The effective indices of the fundamental mode and the second mode

Mode's $n_{eff}$		Fundamental mode(inner core mode)	Second mode(outer core mode)
$\lambda/\mu\text{m}$			
$\lambda < \lambda_p$	1.40	1.357128	1.351302
	1.45	1.351512	1.347497
	1.50	1.345880	1.343768
Mode's $n_{eff}$		Fundamental mode(outer core mode)	Second mode(inner core mode)
$\lambda/\mu\text{m}$			
$\lambda \geq \lambda_p$	1.55	1.340537	1.339767
	1.60	1.336673	1.334332
	1.65	1.333127	1.328633

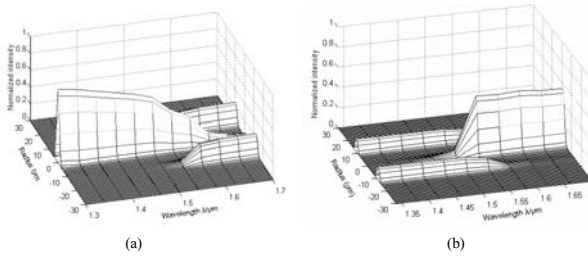


FIG. 4: Normalized intensities of (a) the fundamental mode and (b) the second mode as function of wavelength.

Fig. 4 is relations of normalized intensities of the fundamental mode and the second mode versus wavelength. It can be seen from Fig.4(a) that, at wavelengths shorter than  $\lambda_p$ , the field is essentially confined to the inner core and the field pattern is a Gaussian shape. It matches that in the common transmission fibers. However, when wavelengths longer than  $\lambda_p$ , most of the power of the fundamental mode spreads to the outer core and is effectively guided in the outer core. The mode field pattern is annular shape. As to Fig.4 (b), when  $\lambda < \lambda_p$ , the field is essentially confined to the outer core and is maximal in the outer core. While, when  $\lambda > \lambda_p$ , the field is turn to the inner core, and the shape becomes Gaussian shape. However, the indices of mode guided in the inner core are smaller than those of outer core. So the mode guided in the outer core is the fundamental mode.

Base on above results, we can find that around  $\lambda_p$ , due to optical coupling takes place between the fundamental mode and the second mode, the effective indices of these two modes have varied largely. It results in large D value at  $\lambda_p$ , for both fundamental mode and second mode, as shown in Fig. 5. The two curves are very symmetric due to the coupling between the two modes. Around  $1.55\mu\text{m}$ , D of the fundamental mode reaches about  $-5850 \text{ ps/km/nm}$ , while D of the second mode reaches about  $5850 \text{ ps/km/nm}$ .

Theoretically, there are more than two modes guided in the fibers. Hence, we should make a selective excitation of

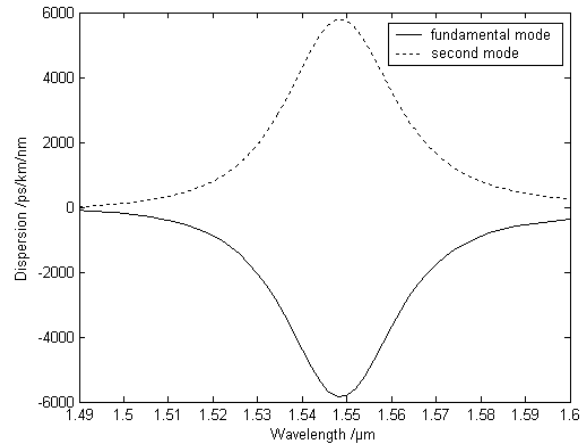


FIG. 5: Dispersion of the fundamental and second modes.

the DCCPCF. So the fundamental mode is selected because it yields a large negative chromatic dispersion. However, in practice, when light is launched into the fiber, the high modes including second mode suffer a high transmission loss with propagation and virtually becomes extinct within a short length of the DCCPCF [3].

#### IV. TOLERANCES ON THE STRUCTURAL PARAMETERS

During the fabrication, the values of structural parameters would have some deviations from the values of the theoretical design inevitably. Therefore the influence of the chromatic dispersion of the fiber with the deviations of the structural parameters were extensively investigated. The effect of possible tolerances in  $d_1, d_2$  is demonstrated in Fig. 6.

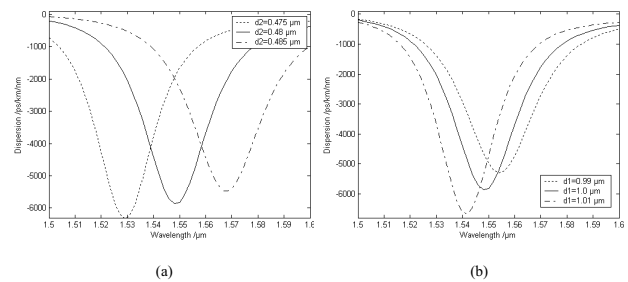


FIG. 6: The dispersion curves of DCCPCF; (a) Keeping fixed  $\Lambda$  and  $d_1$ , for different  $d_2$ ; (b) Keeping fixed  $\Lambda$  and  $d_2$ , for different  $d_1$

Keeping fixed  $\Lambda$  and  $d_1$ , while  $d_2$  is varied with 0.475, 0.48, 0.485  $\mu\text{m}$ , the dispersion curves of DCCPCF is shown in Fig. 6(a). It is apparent from Fig. 6(a) that, by increasing  $d_2$ , the minimum dispersion wavelength shifts to longer wavelength side and the value of the absolute magnitude of dispersion coefficient decreases simultaneously. Similarly, keeping fixed  $\Lambda$  and  $d_2$ , while  $d_1$  is varied with 0.99, 1.0, 1.01  $\mu\text{m}$ , the dispersion curves of DCCPCF is shown in Fig.6 (b). However, from Fig.6 (b) it can be seen that by

increasing  $d_1$ , the minimum dispersion wavelength shifts to shorter wavelength side and the value of the absolute magnitude of dispersion coefficient increases simultaneously. By comparing with Fig. 6(a) and (b), the dispersion changing trends with  $d_1$  and  $d_2$  are quite on the contrary. Simulations also show that 1% variation in  $d_1$  and  $d_2$ , changes  $\lambda_p$  by 1.2% and 0.5%, respectively. Hence, with the acceptable tolerance, there is very little impact on the dispersion curve of the fundamental mode. Therefore, with the result, the designed fiber can be fabricated easily.

## V. CONCLUSION

Based on multipole method, a DCCPCF composed of pure silica and air is investigated thoroughly in this paper. Around 1.55  $\mu\text{m}$ , it exhibits a negative chromatic dispersion as high

as -5850 ps/km/nm. The chromatic dispersion and propagation characteristics of DCCPCF have been simulated systematically. The explanations to propagation states of the fundamental mode and the second mode are given elaborately. Finally, the variation of structural parameters is investigated to evaluate the tolerance of the fabrication. As a result, the designed fiber can be fabricated easily.

## ACKNOWLEDGEMENTS

This work was supported by the State Key Development Program for Basic Research of China under Grant No. 2003CB314905 and the State Key Program of National Natural Science of China under Grant No. 60637010. The authors are grateful to the referees for their helpful comments.

- 
- [1] L.G. Nielsen, S.N. Knudsen, B. Edvold, T. Veng, D. Magnussen, C. C. Larsen, and H. Damsgaard, *Optical Fiber Technology* **6**, 64 (2000).
  - [2] A.J. Antos and D. K. Smith, *Lightwave Technol* **12**, 1739 (1994).
  - [3] J.L. Auguste, J. M. Blondy, J. Maury, J. Marcou, B. Dussardier, G. Monnom, R. Jindal, K. Thyagarajan, and B. P. pal, *Optical Fiber Technology* **8**, 89 (2002).
  - [4] P.P. Bishnu and P. Kamna, *Opt. Commun.* **201**, 335 (2002).
  - [5] J.L. Auguste, R. Jindal, and J. M. Blondy, *Electron. Lett.* **36**, 1689 (2000).
  - [6] K. Thyagarajan, R. K. Varshney, P. Palai, A. K. Ghatak, and I. C. Goyal, *IEEE Photon. Technol. Lett.* **8**, 1510 (1996).
  - [7] F. Gerome, J. L. Auguste, and J. M. Blondy, *Opt. Lett.* **29**, 2725 (2004).
  - [8] F. Gerome, J. L. Auguste, and J. M. Blondy, *Optical Fiber Communication Conference* **2**, 22 (2004).
  - [9] A. Huttunen and P. Torma, *Opt. Express* **13**, 627 (2005).
  - [10] T. Fujisawa, K. Saitoh, K. Wada, and M. Koshiba, *Opt. Express* **14**, 893 (2006).
  - [11] S.G. Yang, Y. J. Zhang, X. Z. Peng, Y. Lu, S. Z. Xie, J. Y. Li, W. Chen, Z. W. Jiang, J. G. Peng, and H. Q. Li, *Opt. Express* **14**, 3015 (2006).
  - [12] Y. Ni, L. Zhang Lei, L. An, J. D. Peng, and C. C. Fan, *IEEE Photon. Technol. Lett.* **16**, 1516 (2004).
  - [13] T.P. White, B.T. Kuhlmeiy, R.C. McPhedran, D. Maystre, G. Renversez, C. M. Sterke, and L. C. Botten, *Journal of the Optical Society of America B* **19**, 2322 (2002).
  - [14] B.T. Kuhlmeiy, T.P. White, G. Renversez, D. Maystre, L. C. Botten, C. M. Sterke, and R.C. McPhedran, *Journal of the Optical Society of America B* **19**, 2331 (2002).